

INTEGRAL OPTICS

https://doi.org/10.1070/QEL16710

Conversion of spectral characteristics of laser radiation in periodic domain structures written by the electron-beam method in planar waveguides formed by Ti diffusion in *Y*-oriented $LiNbO_3$

S.M. Shandarov, L.S. Kokhanchik, T.R. Volk, E.N. Savchenkov, M.V. Borodin

Abstract. **Periodic domain structures for nonlinear conversion of spectral characteristics of laser radiation in the planar Ti : $LiNbO_3$ waveguide have been formed by the method of electron-beam writing. Domain gratings with a spatial period of 6.50 μm formed in the *Y*-cut plate over a wide range of accelerating voltages have been visualised by the method of second harmonic generation microscopy (SHG-microscopy) in transmitting geometry and at waveguide excitation. It is found that the domain structure written at an accelerating voltage of 10 kV in a waveguide with an exponential refractive index profile and an effective thickness of 1.75 μm is characterised by high homogeneity. It is composed of continuous domain rows and provides near-quasi-phase-matching radiation conversion at a wavelength of 1053 nm into the second harmonic for the $TE_0 \rightarrow TE_1$ waveguide process.**

Keywords: *periodic domain structures, diffusion planar waveguide, lithium niobate, SHG microscopy, waveguide quasi-phase-matching SHG.*

1. Introduction

Domain structures with specified parameters in nonlinear optical ferroelectrics make it possible to implement with high efficiency both the frequency conversion of laser radiation in the phase quasi-phase-matched regime [1, 2] and the electro-optical control over its temporal and spatial characteristics [2–4]. A series of advantages of the quasi-phase-matched nonlinear conversion in comparison with the regime of ordinary phase matching, and in particular, the absence of fundamental limitations on the spectral region of the radiation being converted, gave an impetus to an active search for the ways of formation of regular domain structures with a given configuration (see, for example, [2]). A promising method is electron-beam domain writing. This approach has certain advantages over the conventional field method which consists in the formation of domain structures by applying an external field to a system of electrodes deposited on the polar surface of a crystal [5]. Among the advantages of electron-beam writing are the possibility of the formation of the small-size structures down to the submicron size, and also the absence of reverse switching, the suppression of which requires the development of complex regimes of varying the applied voltage when using the field method. Electron-beam formation, in contrast to the field one, allows the domain writing on the nonpolar surfaces of a ferroelectric.

In recent years, we have performed a complex of studies on electron-beam domain writing on the nonpolar *X*- and *Y*-cuts of $LiNbO_3$ [6–16]. The present work is a continuation of these studies as applied to a waveguide formed by Ti diffusion in $LiNbO_3$ (Ti : $LiNbO_3$ waveguide) on the nonpolar *Y*-surface. In the literature, the formation of domains by electron irradiation of polar surfaces, when the domains arising at the irradiation points axially sprout into the crystal depth along the polar axis, is discussed in more detail. A review of the relevant bibliography is beyond the scope of this article; some references can be found, for example, in [5, 15, 16]. On the whole, the use of the discussed method of implementing the devices of integrated photonics [4, 17–21] in combination with the capabilities of electron-beam lithography is particularly attractive.

The base material for optical integrated circuits of quantum photonics, telecommunication, and sensory systems based on nonlinear spectral transformations and electro-optical modulation of laser radiation is lithium niobate [18, 22]. High-quality optical waveguides H^+ : $LiNbO_3$ and Ti : $LiNbO_3$ with conserved nonlinear and electro-optical properties of the substrate material can be formed on its polar and nonpolar cuts by proton exchange and high-temperature diffusion of titanium, respectively [18, 23]. In optical circuits and devices employing the maximum component of light field's waveguide modes, which is parallel to the substrate surface, the use of nonpolar cuts of lithium niobate is more preferable.

In works [7, 8], we have conducted the first studies on electron-beam domain writing in Ti : $LiNbO_3$ waveguides formed on the *Y*-orientated substrates. The results obtained with the accelerating voltage $U = 25$ kV of a scanning electron microscope (SEM) revealed a number of differences in writing characteristics in waveguides compared to the previously established regularities of electron-beam writing in the bulk $LiNbO_3$ crystals of the same (congruent) composition. The specificity of domain formation in the waveguide layers required further studies, primarily by varying the regimes of irradiation, i.e. SEM accelerating voltages and irradiation doses.

Based on the complex of works we have performed in recent years with the use of probe microscopy and confocal

S.M. Shandarov, E.N. Savchenkov, M.V. Borodin Tomsk State University of Control Systems and Radioelectronics, prosp. Lenina 40, 634050 Tomsk, Russia; e-mail: stanislavshandarov@gmail.com;
L.S. Kokhanchik Institute of Microelectronics Technology and High-Purity Materials, Russian Academy of Sciences, ul. Akad. Osip'yana 6, 142432 Chernogolovka, Moscow region, Russia;
T.R. Volk A.V. Shubnikov Institute of Crystallography, Federal Scientific Research Centre 'Crystallography and Photonics', Russian Academy of Sciences, Leninsky prosp. 59, Russia, 119333 Moscow, Russia

Received 24 April 2018; revision received 21 June 2018
Kvantovaya Elektronika **48** (8) 761–766 (2018)
Translated by M.A. Monastyrskiy

SHG-microscopy [10–13], we have developed an approach to completely characterise the process of electron-beam domain writing on the nonpolar surfaces of $LiNbO_3$, and to unambiguously associate the characteristics of the recorded structures with irradiation conditions. The applicability of this approach to waveguide structures was demonstrated using planar waveguides formed by the method of He implantation on the nonpolar surfaces of $LiNbO_3$ [14].

The aim of this work is to study the electron-beam writing of domain gratings in the planar Ti:$LiNbO_3$ waveguide on the nonpolar surface over a wide range of accelerating voltages, to analyse the nature of the specifics of this writing, revealed earlier [7, 8] in the framework of the approach developed in [9–13], and to formulate criteria for selecting optimal conditions for electron-beam domain writing as applied to waveguide structures.

2. Methods for the formation and optical diagnostics of optical waveguides and domain structures

In our experiments, we used a planar waveguide formed by high-temperature Ti diffusion in the air on an optically polished *Y*-cut substrate from congruent lithium niobate measuring 27, 3, and 7 mm along the *X*, *Y*, and *Z* axes, respectively. Input and output of radiation to measure the spectrum of effective refractive indices $n^*_{m\lambda} = n^*_m(\lambda)$ for waveguide TE_m modes ($m = 0, 1, 2$ ... is the mode number) at wavelengths λ = 526.5, 632.8, and 1053 nm, and also for the implementation of waveguide generation of the second optical harmonic, was performed by the coupling prisms made of rutile. The analysis of the measured $n^*_{m\lambda}$ spectra using the known dispersion equation for asymmetric gradient waveguides in the WKB approximation [24] showed that the distribution profiles of the extraordinary refractive index for a given waveguide in depth (along the *y* axis) can be approximated with satisfactory accuracy by the function

$$n_{e\lambda}(y) = n_{es\lambda} + \Delta n_{e\lambda}\exp\left(-\frac{y}{h}\right), \quad y \geqslant 0, \tag{1}$$

with parameter h = 1.75 μm, substrate refractive indices $n_{es\lambda}$ = 2.1476, 2.2028, and 2.2259 and their maximum increments $\Delta n_{e\lambda}$ = 0.0166, 0.0228, and 0.0277 for λ = 1053, 632.8, and 526.5 nm, respectively.

The linear relationship between the refractive index increment in the lithium niobate waveguides and the titanium concentration C_{Ti} is determined at λ = 632.8 nm by the coefficient $dn_e/dC_{Ti} = 1.6\times10^{-29}$ m^{-3} [25]. This allows us to estimate the maximum concentration of titanium (1.43×10^{21} cm^{-3} ≈ 7.6 at %) and, using relation (1), calculate the C_{Ti} distribution in the waveguide layer, shown in Fig. 1a. In the case of $\Delta n_{e\lambda} \ll n_{es\lambda}$ for the asymmetric exponential profile (1) under consideration and the air cover medium, we can neglect the small value of the waveguide mode's light field at the boundary y = 0 and use the known analytical solution of the wave equation for TE modes [26]:

$$E_z^{(m\lambda)}(y) = E_0^{(m\lambda)} J_{\nu_{m\lambda}}\left(V_\lambda \exp\left(-\frac{y}{2h}\right)\right), \quad y \geqslant 0, \tag{2}$$

where $J_{\nu_{m\lambda}}(\xi)$ is the first kind Bessel function with fractional order $\nu_{m\lambda} = (4\pi h/\lambda)\sqrt{(n^*_{m\lambda})^2 - (n_{es\lambda})^2}$; and $V_\lambda = (2\pi h/\lambda)\times\sqrt{2n_{es\lambda}\Delta n_{e\lambda}}$ is the normalised waveguide thickness. Figure 1 shows the results of calculating the distributions of the light fields of the TE_0 and TE_1 waveguide modes at λ_1 = 1053 nm, and also of the TE_0, TE_1, and TE_2 waveguide modes at λ_2 = 526.5 nm, the amplitudes of which $E_0^{(m\lambda)}$ are normalised to the unit power of radiation transferred in a planar waveguide of unit width. It can be seen that the SHG maximum efficiency in this waveguide can be achieved by pumping the TE_0 mode by radiation at λ_1 = 1053 nm, for which the maximum intensity is localised at a depth of ~1.6 μm.

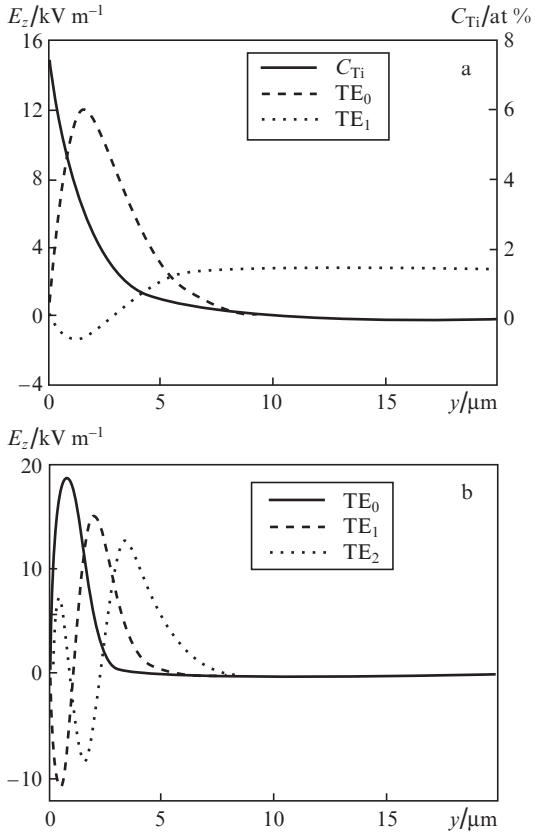

Figure 1. In-depth distributions in the Ti:$LiNbO_3$ waveguide (along the *y* axis) of E_z fields for the TE_0 and TE_1 pump wave modes (λ_1 = 1053 nm) and titanium concentration C_{Ti} (a), and also of the fields of the TE_0, TE_1, and TE_2 second harmonic modes (b).

As a result of good overlap of the fundamental radiation of the TE_0 mode (λ_1 = 1053 nm) with the light fields of TE_0, TE_1, and TE_2 modes at λ = 526.5 nm, which is observed up to a depth of ~5 μm (Fig. 1), effective waveguide quasi-phase-matching conversion into the second harmonic is possible for each of the processes $TE_0 \rightarrow TE_0$, TE_1, and TE_2. To implement the exact first-order quasi-phase-matching for one of them, the ferroelectric domain structure must have a single spatial period defined by the relation [7]

$$\Lambda_{mp} = \frac{\lambda_1}{2(n^*_{p\lambda_2} - n^*_{m\lambda_1})}, \tag{3}$$

where the subscript p is the second harmonic mode number. From the measured values of effective refractive indices $n^*_{m\lambda}$, the required values of the spatial periods Λ_{00} = 5.88 μm, Λ_{01} = 6.60 μm, and Λ_{02} = 6.74 μm were found.

By means of electron-beam method, domain gratings with a spatial period $\Lambda = 6.50$ μm being closest to the calculated value of Λ_{01} were written on the waveguide surface. Let us briefly describe the process of electron-beam domain writing on nonpolar surfaces of a ferroelectric, schematically presented in Fig. 2; a detailed description of this process and the results obtained for $LiNbO_3$ can be found in [7–13, 16]. Local (point) irradiation of a nonpolar surface at the irradiation point nucleates a domain that sprouts along the polar axis (beyond the irradiation region) in a thin surface layer. The driving force behind the growth of this planar domain is the tangential component of the spatial charge field $E_z(r)$ (r is the distance from the charge) formed by the electron beam in the irradiation region; the process of the emergence of a single planar domain is illustrated in Fig. 2a. Domains sprouting from the adjacent irradiation points along the Z axis coalesce, forming a linear extended domain. With the two-dimensional step-by-step displacement of the electron beam in the irradiated plane (in this case, along the Z and X axes), a domain grating is written, with a period Λ given by the distance between the irradiated points along the X axis (Fig. 2b).

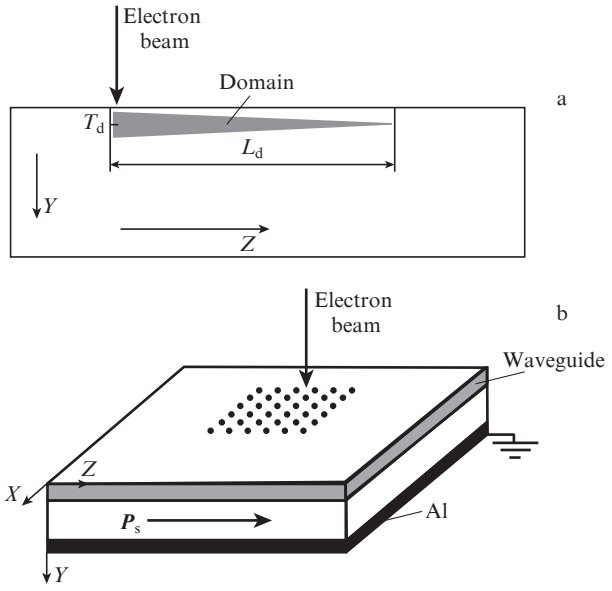

Figure 2. (a) Scheme of the formation of a single domain in the surface region and (b) the method of electron-beam writing of the domain gratings with a spatial period Λ for the planar waveguide $Ti:LiNbO_3$ on nonpolar Y-cut (T_d and L_d are the nucleation depth and individual domain length; $\boldsymbol{P}_s$ is the spontaneous polarisation vector).

The domain gratings were written using a JSM-840A scanning electron microscope with an additional built-in NanoMaker programme which allowed the radiation dose and electron beam movement to be controlled. The following writing regimes were used: the SEM accelerating voltage $U =$ 7, 10, 15, and 25 kV; for all U values, the beam current $I =$ 100 pA at the exposure time $t_e = 150$ ms and the constant area of a single local irradiation region, $S = 0.5$ μm^2, which corresponds to a charge dose $D = It_e/S = 3$ mC cm^{-2} introduced at this local point. The gratings were written by the two-dimensional step-by-step displacement of the electron beam, mentioned above (Fig. 2b). The reverse surface of the sample was metallised by applying an Al film and grounded. The distance between the irradiation points along the crystallographic X axis, equal to 6.5 μm, determined the period Λ of the gratings having been written, while the distance between the irradiation points along the Z axis, equal to 15 μm, ensured the continuity of the corresponding domains. For all U values, the irradiation region size was 385 and 435 μm along the X and Z axes, respectively.

The Nd:YLF laser generating pulses of 10 ns duration at $\lambda = 1053$ nm with an output energy of 170 μJ and a repetition rate of 1 kHz was used for nonlinear-optical diagnostics of the written structures. Domain gratings were visualised by the method of SHG-microscopy in transmission regime using the technique described in detail in [7, 8]. In this case, the Y-surface of the $Ti:LiNbO_3$ waveguide was illuminated by a collimated beam with a polarisation vector oriented along the polar axis (beam aperture from 1 to 3 mm). The pump radiation transmitted through the sample was attenuated by the SZS-21 and SZS-9 filters, which allowed the image of the gratings to be recorded owing to the scattered second-harmonic radiation generated on them. The recording system consisted of a lens with magnification from 2.8$^\times$ to 10$^\times$ and a DCM 310 video eyepiece. In using lenses with magnifications of 2.8$^\times$ and 4$^\times$, a spatial low-pass filter was added to the microscopic system to reduce the second harmonic intensity, which was asynchronously generated in the substrate volume.

To study the waveguide SHG, we used the excitation of the TE_0 and TE_1 modes at $\lambda = 1053$ nm by means of the input rutile prism. The waveguide pump beam had an aperture of about 1 mm and propagated along the X axis in such a way as to pass through one or two of the written gratings (see Fig. 3 below). The SHG was registered by the presence, at the output of the domain structure being investigated, of the waveguide radiation beam at $\lambda_2 = 526.5$ nm, which was visualised as a result of its scattering into radiative modes by focusing the microscopic system described above directly onto the boundary $y = 0$ of the waveguide layer with an air cover medium (see Fig. 1).

To estimate the efficiency of waveguide conversion into the second harmonic and the impact of the propagation direction of the pump beam in the TE_0 mode, the radiation distribution at the waveguide output end face was projected onto the photosensitive area of a calibrated photodetector, which made it possible to measure the peak power of pump radiation, and, using the SZS-21 and SZS-9 attenuating filters, the peak power of the second harmonic. The angle β between the X axis of the crystal and the direction of propagation of the pump beam in the XZ plane of the waveguide layer was determined by the corresponding rotation of the input prism, and took the values 0 and 7°50′.

It should be noted that in all above SHG experiments, the eee-type interaction was used, characterised by a component of the quadratic susceptibility tensor d_{33} having a maximum value in the lithium niobate crystal.

3. Experimental results

Figure 3a shows images of four domain gratings visualised by the SHG-microscopy method. Gratings 1, 2, 3, and 4 were written at accelerating voltages $U =$ 7, 10, 15, and 25 kV, respectively. Figure 3b displays a fragment of the SHG image of structure 2 (Fig. 3a) written at $U = 10$ kV. This fragment demonstrates the grating homogeneity and the correspondence of its period to a given value ($\Lambda = 6.5$ μm), and also evidences that the grating consists virtually of continuous

domain rows. At the same time, the image of structure 1 in Fig. 3a (U = 7 kV), the brightness of which is maximal at the right and left edges and reduced at the centre, indicates its insufficient homogeneity, which is revealed when this transmission technique is used.

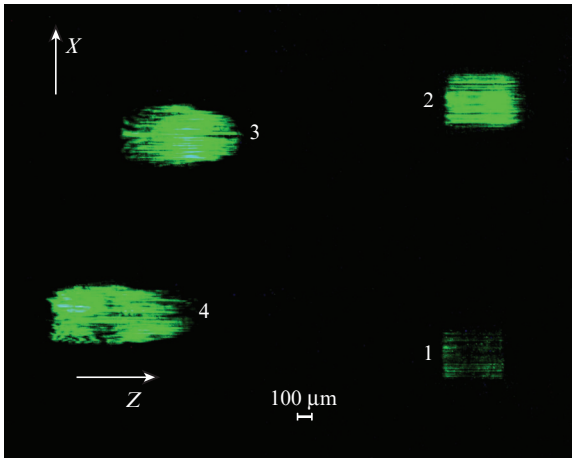

a

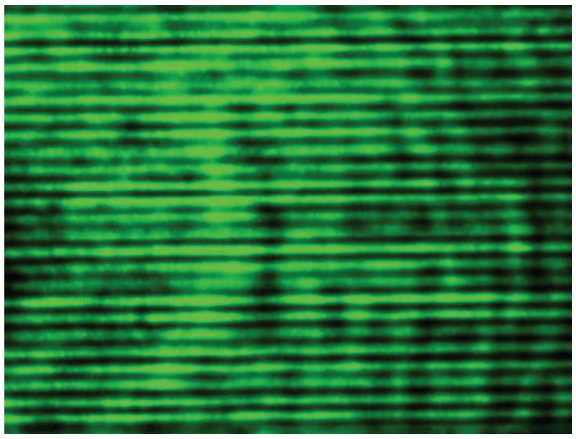

b

Figure 3. (Colour online) (a) Visualisation of periodic domain structures written by electron beam on the surface of a planar Y-oriented Ti:$LiNbO_3$ waveguide at accelerating voltages of (1) 7, (2) 10, (3) 15, and (4) 25 kV with the use of second-harmonic radiation in transmission geometry, and (b) visualisation of a fragment of structure 2.

Figure 4 shows an experimentally observed typical SHG picture in the case of irradiation of gratings 4, 3, and 1 by a pump beam (TE_0 mode). It should be noted that the SHG images of domain structures 1–4 and the generated waveguide radiation beams were not observed in excitation by the pump beam at λ = 526.5 nm (TE_1 waveguide mode). In the case shown in Fig. 4, the pump beam in the first position propagated through grating 4, in the second – through grating 3, and in the third–sequentially through gratings 1 and 2 (Fig. 3a). The waveguide beam of the second harmonic acquires optimal characteristics (significant aperture and high brightness) after passing of the pump beam through structure 2. After passing through structure 1, a narrow second harmonic beam with an aperture of less than 100 μm is observed, which may be due to the good quality of the periodic structure for the waveguide SHG, which is close to quasi-phase-matching in the illuminated region, and not good enough in its other cross sections (cf. with Fig. 3a rotated relative to Fig. 4 by 90°, where the SHG maximum efficiency is attained at the right and left edges of grating 1). The radiation beam at λ_2 = 526.5 nm is absent after passing through structures 3 and 4, which indicates a low efficiency of the waveguide SHG in this case. The SHG images of structures 3 and 4 along the Z axis are clearly bounded and rectangular in shape because they are only registered for the areas through which the pump beam propagates (cf. with Fig. 3a where the images are stretched along the Z axis).

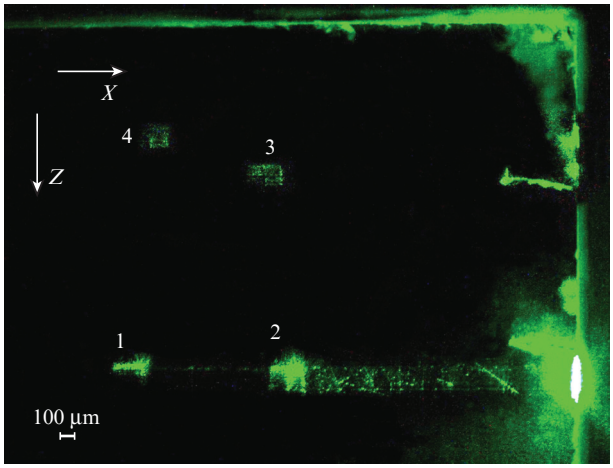

Figure 4. (Colour online) Visualisation of the periodic domain structures 1–4 in waveguide geometry by means of second-harmonic radiation (see Fig. 3), and visualisation of the waveguide beams of radiation with λ_2 = 526.5 nm, generated in structures 1 and 2 in excitation by the beams of pump radiation with λ_1 = 1053 nm (TE_0 mode) propagating from left to right precisely along the X axis of the crystal (at β = 0).

The characteristics of the waveguide SHG obtained in structure 2 indicate that the parameters and homogeneity of this domain grating are optimal for the SHG conversion in this waveguide. The efficiency of the waveguide conversion into the second harmonic in structure 2, which was measured in the pump beam propagation exactly along the X axis (at β = 0) constitutes 1.1×10^{-10} W^{-1}, while it increases up to 6.4×10^{-9} W^{-1} at β = 7°50′. Thus, the electron-beam writing regime of grating 2 provides the best characteristics of the waveguide SHG conversion, and the spatial period Λ = 6.5 μm used in this experiment can ensure the exact fulfilment of the eee-type quasi-phase-matching condition in the waveguide under investigation only when the pump beam propagates at a certain angle to the X axis of the crystal.

4. Discussion of results

Our results demonstrate the possibility of implementing an efficient waveguide SHG in a regular domain structure written by an electron beam. The condition for solving this problem is a controlled selection of the mode of electron-beam writing, which provides optimal conversion characteristics. This conclusion follows from a comparison of the results obtained in transmission and waveguide geometries: the SHG in transmission geometry is observed in all the gratings having been written (Fig. 3), regardless of the accelerating voltage magnitude, whereas the waveguide SHG is only detected in gratings 1 and 2 written at U = 7 and 10 kV (Fig. 4).

The choice of conditions for electron-beam domain writing is based on the approach developed in [10–13]. In these studies it was shown that, in electron irradiation of nonpolar surface of a ferroelectric, the depth T_d of nucleation of isolated domains is determined by the equilibrium path depth R_e of primary electrons, which is described by the general power law

$$R_e = \frac{A W_0^k}{\rho}, \tag{4}$$

where W_0 is the energy of electrons in the beam; and ρ is the crystal density. The values of the exponent k and dimensionless coefficient A given in the literature for $LiNbO_3$ have a large scatter. Nevertheless, based on a comparison of the experimental estimates for T_d obtained by chemical etching and the calculated R_e values using the literature data for k and A, it was shown that the expression

$$T_d \approx R_e = \frac{78.9 U^{1.7}}{\rho} \tag{5}$$

describes with satisfactory accuracy the dependence of the T_d value (in μm) on the acceleration voltage U (in kV) for lithium niobate samples of congruent composition with $\rho = 4.65\times10^3$ kg m^{-3}. Thus, with the use of this expression, it is possible to determine the domain nucleation depth by varying U or to estimate its value.

The T_d values calculated from formula (5) for the interval of accelerating voltages, including the values used in our experiment, are given in Table 1. As noted above, the visualisation of the generated second harmonic beams in the waveguide geometry, related to its scattering into radiative modes, is realised only on gratings 1 and 2 written at $U = 7$ and 10 kV (Fig. 4). According to Table 1, the domain nucleation depth for these gratings does not exceed 1 μm, whereas for structure 2 it is equal to 0.85 μm, which is closest to the position of a single maximum of the light field of the TE_0 mode and the position of the first maximum of the TE_1 mode (about 0.7 and 0.5 μm from the boundary with a cover medium, respectively, see Fig. 1) at $\lambda_2 = 526.5$ nm. Thus, gratings at $U = 7$ and 10 kV are written within the region of a good overlap of the fields of the TE_0 mode of the pump beam and TE_0 and TE_1 modes of the second harmonic, which can provide a noticeable efficiency of nonlinear $TE_0 \rightarrow TE_0$ or $TE_0 \rightarrow TE_1$ conversion, depending on the implementation of quasi-phase-matching conditions. Gratings 3 and 4 have been written at $U = 15$ and 25 kV at a depth of 1.7 μm or more, where the pump field amplitude for TE_0 modes is close to its maximum value $E_{max}^{(\lambda_1)}$ (Fig. 1a), whereas the amplitude is less than $0.3E_{max}^{(\lambda_2)}$ at the second harmonic wavelength (Fig. 1b). The field of the TE_1 mode of the second harmonic in the range $0 \leqslant y \leqslant 1.7$ μm has a sign-alternating character, and its overlap integral with the field of the TE_0 mode of the pump beam in this range should be substantially less than that in the interval $0 \leqslant y \leqslant 0.85$ μm.

Table 1. The domain nucleation depth T_d on the nonpolar Y-cut of congruent lithium niobate in electron-beam writing for various accelerating voltages U.

U/kV	T_d/μm	U/kV	T_d/μm
5	0.26	15	1.7
7	0.46	20	2.8
10	0.85	25	4.0

Therefore, the images of gratings 3 and 4 in the waveguide geometry (Fig. 4) are only observed because of the scattering of radiation with a wavelength of λ_2 into radiative modes. Similar results were obtained by us earlier for electron-beam domain writing in the waveguides implanted by He atoms on the nonpolar surface of congruent lithium niobate [14].

The results obtained, together with the results of work [14], indicate the possibility of fitting the depth T_d of the domain structure having been written (Table 1) to the localisation depth of the light field of waveguide modes by selecting the accelerating voltage U with the use of expression (5). In the present paper, it is shown that such a fitting provides optimal characteristics of the waveguide SHG conversion in the Y-oriented Ti : $LiNbO_3$ waveguide.

It is necessary to comment on the difference in shape of the 'deep' gratings 3 and 4 written at $U = 15$ and 25 kV from the 'shallower' structures 1 and 2, which is observed in the transmitted light (Fig. 3a). For the waveguide under study, the Ti concentration does not exceed 3 at% for the region where the domains are written at $U = 15$ kV, while at $U = 25$ kV the domains are formed in a layer with a minimum concentration $C_{Ti} \leqslant 0.8$ at% (see Fig. 1a and Table 1). Gratings 3 and 4 have a longer length along the Z axis and an oval shape. As shown in [9], this is due to the additivity of the spatial charge fields $\boldsymbol{E}_i$ induced by the electron beam within the irradiation zones. Because of the exceptionally low conductivity of congruent lithium niobate ($G = 10^{-16} - 10^{-18}\ \Omega^{-1}$ cm^{-1}), the fields $\boldsymbol{E}_i$ decay during the time $\tau_M = \varepsilon\varepsilon_0/G > 10^4 - 10^6$ s (where $\varepsilon\varepsilon_0$ is permittivity), which is an order of magnitude longer than the grating writing time (minutes). Thus, the grating is written in the total field

$$\boldsymbol{E} = \sum_{i=1}^{n} \boldsymbol{E}_i .$$

The shape of the written structures (in our case, structures 3 and 4) is determined by the distribution of this total field along the Z axis.

The undistorted shape of gratings 1 and 2 written within the Ti layer with a concentration exceeding 4.6 at% (see Table 1 and Fig. 1a) indicates that there is no impact of additivity of the fields $\boldsymbol{E}_i$ on the grating shape, which is explained by an increase in conductivity in the specified layer. The increase in lithium niobate conductivity when doping by transition metal impurities is mentioned in the literature [5]. By the example of reconstructed $LiNbO_3$, we have shown [15] that the additivity effect of the fields $\boldsymbol{E}_i$ is absent when the conductivity G is increased, since in this case the grating shape is not distorted. In addition, an increase in G leads to an increase in the D_{thr} threshold dose for domain formation. Indeed, Kokhanchik et al. [7] noted an increase in the D_{thr} dose in the Ti:$LiNbO_3$ waveguide. A similar effect was observed for electron-beam domain writing on the polar surface in the same waveguide [27].

The estimates of the dependence of the waveguide conversion efficiency of pump radiation into the second harmonic on the angle between the pump beam and the X axis of the crystal, obtained on the basis of experimental data, show that the efficiency can reach 1.1×10^{-8} W^{-1} for the $TE_0 \rightarrow TE_1$ process in the domain grating 2 of the waveguide under investigation at the optimum angle $\beta = 9°40'$ corresponding to precise fulfilment of the quasi-phase-matching condition. For the $TE_0 \rightarrow TE_0$ process, the overlap integral of the modes' fields in this structure approximately twofold exceeds that for the $TE_0 \rightarrow$

TE_1 process. However, the factor that determines a decrease in the $TE_0 \rightarrow TE_0$ conversion efficiency due to a deviation from the quasi-phase-matching condition is just 0.0014 at the optimum angle $\beta = 5°57'$.

5. Conclusions

The electron-beam writing of periodic domain structures in a planar waveguide formed by high-temperature diffusion of Ti in $LiNbO_3$ on a nonpolar *Y*-cut at SEM accelerating voltages from 7 to 25 kV has been investigated. From the analysis of the measured spectra of effective refractive indices of the waveguide TE modes, it was established that the distributions of the refractive index increment of the waveguide layer and Ti concentration can be approximated by an exponential function with the parameter $h = 1.75$ μm, while the implementation of quasi-phase-matching SHG in the waveguide pumping by radiation with a wavelength of 1053 nm (TE_0 mode) is possible in domain gratings with spatial periods from 5.88 to 6.74 μm. The domain gratings with a period $\Lambda = 6.50$ μm, formed by the electron-beam method, were visualised by the method of SHG-microscopy both in the transmission regime and at waveguide excitation. It is established that the domain structure written at an accelerating voltage of 10 kV is characterised by high homogeneity, consists of continuous domain rows and provides the best SHG conversion for the $TE_0 \rightarrow TE_1$ waveguide process, which is relatively close to the quasi-phase-matching. Our analysis of the conditions of electron-beam domain writing, based on the approach developed in [10–15], indicates the possibility of fitting the depth of the domain structure being written to the localisation depth of the light field of interacting waveguide modes by selecting the optimal accelerating voltage *U*.

Acknowledgements. This work was supported by the Russian Foundation for Basic Research (Grant Nos 16-29-14046-ofi_m, 16-29-11777-ofi_m, and 16-02-00439_a). The studies on visualisation of the second harmonic of domain structures in transmission geometry by radiation, conducted by E.N. Savchenkov, were supported by the Ministry of Education and Science of the Russian Federation for 2017–2019 (State Task No. 3.1110.2017/4.6).

References

1. Myers L.I., Eckardt R.C., Fejer M.M., Byer R.L., Bosenberg W.R., Pierce J.W. *J. Opt. Soc. Am. B*, **12**, 2102 (1995).
2. Ferrari P., Grilli S., DeNatale P. (Eds) *Ferroelectric Crystals for Photonic Applications* (Berlin–Heidelberg: Springer-Verlag, 2009, 2014).
3. Yamada M. *Rev. Sci. Instrum.*, **71**, 4010 (2000).
4. Mhaouech I., Coda V., Montemezzani G., Chauvet M., Guilbert L. *Opt. Lett.*, **41**, 4174 (2016).
5. Volk T., Woehlecke M. *Lithium Niobate: Defects, Photorefraction and Ferroelectric Switching* (Berlin–Heidelberg: Springer-Verlag, 2008).
6. Kokhanchik L.S., Punegov D.V. *Ferroelectrics*, **373**, 69 (2008).
7. Kokhanchik L.S., Borodin M.V., Shandarov S.M., Burimov N.I., Shcherbina V.V., Volk T.R. *Fiz. Tverd. Tela*, **52**, 1602 (2010).
8. Kokhanchik L.S., Borodin M.V., Burimov N.I., Shandarov S.M., Shcherbina V.V., Volk T.R. *IEEE Trans. Ultrason., Ferroelectr. Freq. Control*, **59**, 1076 (2012).
9. Kokhanchik L.S., Volk T.R. *Appl. Phys. B*, **110**, 367 (2013).
10. Kokhanchik L.S., Gainutdinov R.V., Mishina E.D., Lavrov S.D., Volk T.R. *Appl. Phys. Lett.*, **105**, 142901 (2014).
11. Kokhanchik L.S., Gainutdinov R.V., Volk T.R. *Fiz. Tverd. Tela*, **57**, 937 (2015).
12. Kokhanchik L.S., Gainutdinov R.V., Lavrov S.D., Mishina E.D., Volk T.R. *Ferroelectrics*, **480**, 49 (2015).
13. Kokhanchik L.S., Gainutdinov R.V., Lavrov S.D., Volk T.R. *J. Appl. Phys.*, **118**, 072001 (2015).
14. Volk T.R., Kokhanchik L.S., Gainutdinov R.V., Bodnarchuk Ya.V., Shandarov S.M., Borodin M.V., Lavrov S D., Liu H.L., Chen F. *J. Lightwave Technol.*, **33**, 4761 (2015).
15. Kokhanchik L.S., Bodnarchuk Ya.V.,Volk T.R. *J. Appl. Phys.*, **122**, 104105 (2017).
16. Volk T.R., Kokhanchik L.S., Gainutdinov R.V., Bodnarchuk Ya.V., Lavrov S.D. *J. Adv. Dielectrics*, **8**, 1830001 (2018).
17. Tanzilli S., Tittel W., De Riedmatten H., Zbinden H., Baldi P., De Micheli M., Ostrovsky D.B., Gisin N. *Eur. Phys. J. D*, **18**, 155 (2002).
18. Alibart O., D'Auria V., De Micheli M., Doutre F., Kaiser F., Labonté L., Lunghi T., Picholle É., Tanzilli S. *J. Opt.*, **18**, 104001 (2016).
19. Arahira S., Murai H., Sasaki H. *Opt. Express*, **24**, 19581 (2016).
20. Bock M., Lenhard A., Chunnilall C., Becher C. *Opt. Express*, **24**, 23992 (2016).
21. Hickstein D.D., Carlson D.R., Kowligy A., Kirchner M., Domingue S.D., Nader N., Timmers H., Lind A., Ycas G.G., Murnane M.M., Kapteyn H.C., Papp S.B., Diddams S.A. *Optica*, **4**, 1538 (2017).
22. Janner D., Tulli D., Garcia-Granda M., Belmonte M., Pruneri V. *Laser Photonics Rev.*, **3**, 301 (2009).
23. Bazzan M., Sada C. *Appl. Phys. Rev.*, **2**, 040603 (2015).
24. Sychugov V.A., Ctyroky J. *Sov. J. Quantum Electron.*, **12**, 392 (1982) [*Kvantovaya Elektron.*, **9**, 634 (1982)].
25. Schmidt R.V., Kaminov I.P. *Appl. Phys. Lett.*, **25**, 458 (1974).
26. Tamir T. (Ed.) *Guided-Wave Optoelectronics* (Springer Series in Electronics and Photonics, 1988).
27. Restoin C., Darraud-Taupiac C., Decossas J.-L., Vareille J.-C., Couderc V., Barthelemy A., Martinez A., Hauden J. *Appl. Opt.*, **40**, 6056 (2001).